

AD-A079 308

ELECTROMECHANICAL SYSTEMS OF NEW MEXICO INC ALBUQUERQUE F/6 8/13

DYNAMIC STRESS-STRAIN MEASUREMENTS ON MISERS BLUFF. (U)

MAY 79 R A SHUNK

DNA001-78-C-0260

UNCLASSIFIED

ESI-79-002-TR

DNA-4970T

NL

1 of 1
All
AD-A079 308

END
DATE
F/6 8/13
2-80
REC

AD-E300 637

13
DNA 4970T

DYNAMIC STRESS-STRAIN MEASUREMENTS ON MISERS BLUFF

ADA 079308

Electromechanical Systems of New Mexico, Inc.
P.O. Box 11730
Albuquerque, New Mexico 87192

1 May 1979

Topical Report for Period 1 May 1978–30 April 1979

CONTRACT No. DNA 001-78-C-0260

APPROVED FOR PUBLIC RELEASE;
DISTRIBUTION UNLIMITED.

THIS WORK SPONSORED BY THE DEFENSE NUCLEAR AGENCY
UNDER RDT&E RMSS CODE B344079462 J11AAXSX35257 H2590D.

DDC FILE COPY
Prepared for
Director
DEFENSE NUCLEAR AGENCY
Washington, D. C. 20305

22 5 040

Destroy this report when it is no longer
needed. Do not return to sender.

PLEASE NOTIFY THE DEFENSE NUCLEAR AGENCY,
ATTN: STTI, WASHINGTON, D.C. 20305, IF
YOUR ADDRESS IS INCORRECT, IF YOU WISH TO
BE DELETED FROM THE DISTRIBUTION LIST, OR
IF THE ADDRESSEE IS NO LONGER EMPLOYED BY
YOUR ORGANIZATION.



UNCLASSIFIED

SECURITY CLASSIFICATION OF THIS PAGE (When Data Entered)

11. REPORT DOCUMENTATION PAGE		READ INSTRUCTIONS BEFORE COMPLETING FORM
1. REPORT NUMBER DNA 4970T	2. GOVT ACCESSION NO.	3. RECIPIENT'S CATALOG NUMBER
4. TITLE (and Subtitle) DYNAMIC STRESS-STRAIN MEASUREMENTS ON MISERS BLUFF,		5. TYPE OF REPORT & PERIOD COVERED Topical Report, For Period 1 May 1978-30 April 1979
7. AUTHOR(s) R. A. Shunk		6. PERFORMING ORG. REPORT NUMBER ESI-79-002-TR
9. PERFORMING ORGANIZATION NAME AND ADDRESS Electromechanical Systems of New Mexico, Inc. P.O. Box 11730 Albuquerque, New Mexico 87192		8. CONTRACT OR GRANT NUMBER(s) DNA 001-78-C-0260
11. CONTROLLING OFFICE NAME AND ADDRESS Director Defense Nuclear Agency Washington, D.C. 20305		10. PROGRAM ELEMENT, PROJECT, TASK AREA & WORK UNIT NUMBERS Subtask J11AAXSX352-57
14. MONITORING AGENCY NAME & ADDRESS (if different from Controlling Office) DNA		12. REPORT DATE 1 May 1979
15. SECURITY CLASS (of this report) UNCLASSIFIED		
16. DISTRIBUTION STATEMENT (of this Report) Approved for public release; distribution unlimited.		
17. DISTRIBUTION STATEMENT (of the abstract entered in Block 20, if different from Report)		
18. SUPPLEMENTARY NOTES This work sponsored by the Defense Nuclear Agency under RDT&E RMSS Code B344079462 J11AAXSX35257 H2590D.		
19. KEY WORDS (Continue on reverse side if necessary and identify by block number) Soil Strain Dynamic Soil Strain Strain Gage High Explosives MISERS BLUFF, Phase II		
20. ABSTRACT (Continue on reverse side if necessary and identify by block number) MISERS BLUFF, Phase II, Test 2 was the near simulation explosion of six 120 ton ANFO charges on the corner of a hexagon 100 m on a side. Soil stress and strain measurements at several depths were made 6 m from the array center and between two charges. During the compressive loading by the air blast, dynamic stress-strain curves were plotted where data are available. Comparing the two locations shows different material behavior. Also, the near surface stress gages did not reproduce the air shock structure indicating a peculiarity of the		

DD FORM 1 JAN 73 1473 EDITION OF 1 NOV 65 IS OBSOLETE

UNCLASSIFIED

SECURITY CLASSIFICATION OF THIS PAGE (When Data Entered)

37277

UNCLASSIFIED

SECURITY CLASSIFICATION OF THIS PAGE(When Data Entered)

20. ABSTRACT (Continued)

material or material-gage interaction process. The material in the test bed exhibited a large strain energy absorption for propagating stress waves.

[Handwritten mark]

UNCLASSIFIED

SECURITY CLASSIFICATION OF THIS PAGE(When Data Entered)

PREFACE

The measurements of stress and strain on MISERS BLUFF, Phase II that are discussed here were made by the Waterways Experiment Station under the direction of personnel from the Weapons Effects Laboratory. Mr. Don Day and Mr. Don Murrell have been most helpful in obtaining data and in supervising the installation of the gages in the field. Mr. John Stout did the gage placement which turned out to be more difficult than anticipated because of the lack of a cohesive soil. Operation of the recording facility was done by Mr. Jim Pickens. My thanks to these people and others at WES who were responsible for the successful execution of this part of the experiment. The DNA Test Group Director was LCDR J. D. Strode and the Technical Director was Capt. Robert DeRaad. This work was done under contract to DNA on Contract DNA001-78-C-0260.

Accesision For	Line Gages
1	2
3	4
5	6
7	8
9	10
11	12
13	14
15	16
17	18
19	20
21	22
23	24
25	26
27	28
29	30
31	32
33	34
35	36
37	38
39	40
41	42
43	44
45	46
47	48
49	50
51	52
53	54
55	56
57	58
59	60
61	62
63	64
65	66
67	68
69	70
71	72
73	74
75	76
77	78
79	80
81	82
83	84
85	86
87	88
89	90
91	92
93	94
95	96
97	98
99	100
101	102
103	104
105	106
107	108
109	110
111	112
113	114
115	116
117	118
119	120
121	122
123	124
125	126
127	128
129	130
131	132
133	134
135	136
137	138
139	140
141	142
143	144
145	146
147	148
149	150
151	152
153	154
155	156
157	158
159	160
161	162
163	164
165	166
167	168
169	170
171	172
173	174
175	176
177	178
179	180
181	182
183	184
185	186
187	188
189	190
191	192
193	194
195	196
197	198
199	200
201	202
203	204
205	206
207	208
209	210
211	212
213	214
215	216
217	218
219	220
221	222
223	224
225	226
227	228
229	230
231	232
233	234
235	236
237	238
239	240
241	242
243	244
245	246
247	248
249	250
251	252
253	254
255	256
257	258
259	260
261	262
263	264
265	266
267	268
269	270
271	272
273	274
275	276
277	278
279	280
281	282
283	284
285	286
287	288
289	290
291	292
293	294
295	296
297	298
299	300
301	302
303	304
305	306
307	308
309	310
311	312
313	314
315	316
317	318
319	320
321	322
323	324
325	326
327	328
329	330
331	332
333	334
335	336
337	338
339	340
341	342
343	344
345	346
347	348
349	350
351	352
353	354
355	356
357	358
359	360
361	362
363	364
365	366
367	368
369	370
371	372
373	374
375	376
377	378
379	380
381	382
383	384
385	386
387	388
389	390
391	392
393	394
395	396
397	398
399	400
401	402
403	404
405	406
407	408
409	410
411	412
413	414
415	416
417	418
419	420
421	422
423	424
425	426
427	428
429	4210
4211	4212
4213	4214
4215	4216
4217	4218
4219	4220
4221	4222
4223	4224
4225	4226
4227	4228
4229	4230
4231	4232
4233	4234
4235	4236
4237	4238
4239	4240
4241	4242
4243	4244
4245	4246
4247	4248
4249	4250
4251	4252
4253	4254
4255	4256
4257	4258
4259	4260
4261	4262
4263	4264
4265	4266
4267	4268
4269	4270
4271	4272
4273	4274
4275	4276
4277	4278
4279	4280
4281	4282
4283	4284
4285	4286
4287	4288
4289	4290
4291	4292
4293	4294
4295	4296
4297	4298
4299	4300
4301	4302
4303	4304
4305	4306
4307	4308
4309	4310
4311	4312
4313	4314
4315	4316
4317	4318
4319	4320
4321	4322
4323	4324
4325	4326
4327	4328
4329	4330
4331	4332
4333	4334
4335	4336
4337	4338
4339	4340
4341	4342
4343	4344
4345	4346
4347	4348
4349	4350
4351	4352
4353	4354
4355	4356
4357	4358
4359	4360
4361	4362
4363	4364
4365	4366
4367	4368
4369	4370
4371	4372
4373	4374
4375	4376
4377	4378
4379	4380
4381	4382
4383	4384
4385	4386
4387	4388
4389	4390
4391	4392
4393	4394
4395	4396
4397	4398
4399	4400
4401	4402
4403	4404
4405	4406
4407	4408
4409	4410
4411	4412
4413	4414
4415	4416
4417	4418
4419	4420
4421	4422
4423	4424
4425	4426
4427	4428
4429	4430
4431	4432
4433	4434
4435	4436
4437	4438
4439	4440
4441	4442
4443	4444
4445	4446
4447	4448
4449	4450
4451	4452
4453	4454
4455	4456
4457	4458
4459	4460
4461	4462
4463	4464
4465	4466
4467	4468
4469	4470
4471	4472
4473	4474
4475	4476
4477	4478
4479	4480
4481	4482
4483	4484
4485	4486
4487	4488
4489	4490
4491	4492
4493	4494
4495	4496
4497	4498
4499	4500
4501	4502
4503	4504
4505	4506
4507	4508
4509	4510
4511	4512
4513	4514
4515	4516
4517	4518
4519	4520
4521	4522
4523	4524
4525	4526
4527	4528
4529	4530
4531	4532
4533	4534
4535	4536
4537	4538
4539	4540
4541	4542
4543	4544
4545	4546
4547	4548
4549	4550
4551	4552
4553	4554
4555	4556
4557	4558
4559	4560
4561	4562
4563	4564
4565	4566
4567	4568
4569	4570
4571	4572
4573	4574
4575	4576
4577	4578
4579	4580
4581	4582
4583	4584
4585	4586
4587	4588
4589	4590
4591	4592
4593	4594
4595	4596
4597	4598
4599	4600
4601	4602
4603	4604
4605	4606
4607	4608
4609	4610
4611	4612
4613	4614
4615	4616
4617	4618
4619	4620
4621	4622
4623	4624
4625	4626
4627	4628
4629	4630
4631	4632
4633	4634
4635	4636
4637	4638
4639	4640
4641	4642
4643	4644
4645	4646
4647	4648
4649	4650
4651	4652
4653	4654
4655	4656
4657	4658
4659	4660
4661	4662
4663	4664
4665	4666
4667	4668
4669	4670
4671	4672
4673	4674
4675	4676
4677	4678
4679	4680
4681	4682
4683	4684
4685	4686
4687	4688
4689	4690
4691	4692
4693	4694
4695	4696
4697	4698
4699	4700
4701	4702
4703	4704
4705	4706
4707	4708
4709	4710
4711	4712
4713	4714
4715	4716
4717	4718
4719	4720
4721	4722
4723	4724
4725	4726
4727	4728
4729	4730
4731	4732
4733	4734
4735	4736
4737	4738
4739	4740
4741	4742
4743	4744
4745	4746
4747	4748
4749	4750
4751	4752
4753	4754
4755	4756
4757	4758
4759	4760
4761	4762
4763	4764
4765	4766
4767	4768
4769	4770
4771	4772
4773	4774
4775	4776
4777	4778
4779	4780
4781	4782
4783	4784
4785	4786
4787	4788
4789	4790
4791	4792
4793	4794
4795	4796
4797	4798
4799	4800
4801	4802
4803	4804
4805	4806
4807	4808
4809	4810
4811	4812
4813	4814
4815	4816
4817	4818
4819	4820
4821	4822
4823	4824
4825	4826
4827	4828
4829	4830</td

TABLE OF CONTENTS

<u>Section</u>		<u>Page</u>
I	INTRODUCTION	5
II	DYNAMIC STRESS-STRAIN MEASUREMENTS	7
III	CONCLUSIONS AND RECOMMENDATIONS	10

LIST OF ILLUSTRATIONS

Figure

1	Measurement and charge locations for the stress-strain measurements on Misers Bluff-Phase II. Horizontal stresses are measured in the directions of the arrows at the measurement locations.	6
2	Surface overpressure near the stress-strain measurement locations at 87 m, 240° azimuth.	11
3	Diaphragm stress gages partially uncovered for measuring vertical and horizontal stress.	12
4	Vertical stress at 87 m, 0.3 m depth and 240° azimuth.	13
5	Horizontal stress at 87 m, 0.3 m depth and 240° azimuth.	14
6	Vertical strain at 87 m, 0.3 m depth and 240° azimuth.	15
7	Horizontal stress at 87 m, 0.6 m depth and 240° azimuth	16
8	Vertical strain at 87 m, 0.6 m depth and 240° azimuth.	17
9	Vertical stress at 87 m, 1.2 m depth and 240° azimuth.	18

LIST OF ILLUSTRATIONS (Continued)

<u>Figure</u>		<u>Page</u>
10	Horizontal stress at 87 m, 1.2 m depth and 240 ⁰ azimuth.	19
11	Vertical strain at 87 m, 1.2 m depth and 240 ⁰ azimuth.	20
12	Dynamic stress-strain curves for three depths at 87 m, 240 ⁰ azimuth.	21
13	Air blast wave form at 180 ⁰ and 6 m from center of the array over strain gage emplacement.	22
14	Vertical stress at 6 m, 0.3 m depth and 180 ⁰ azimuth.	23
15	Horizontal stress at 6 m, 0.3 m depth and 180 ⁰ azimuth.	24
16	Horizontal stress at 6 m, 0.6 m depth and 180 ⁰ azimuth.	25
17	Vertical strain from 6 m, 0.6 m depth and 180 ⁰ azimuth.	26
18	Horizontal stress from 6 m, 0.9 m depth and 180 ⁰ azimuth.	27
19	Vertical strain from 6 m, 0.9 m depth and 180 ⁰ azimuth.	28
20	Vertical stress from 6 m, 1.2 m depth and 180 ⁰ azimuth.	29
21	Horizontal stress at 6 m, 1.2 m depth and 180 ⁰ azimuth.	30
22	Vertical strain at 6 m, 1.2 m depth and 180 ⁰ azimuth.	31
23	Dynamic stress-strain curves for three depths at 6 m, 180 ⁰ azimuth.	32

SECTION I
INTRODUCTION

MISERS BLUFF, Phase II, Test 2 was the near simultaneous explosion of six 120 ton ANFO charges on the corners of a hexagon 100 m on a side. The details of the experiment are described in Reference 1.

There were stress and strain measurements made at three places in the test bed and at several depths shown in Figure 1 (Reference 2). The comparison of stress and strain at the same time at the same depth will produce a dynamic stress-strain curve of the material reaction. The resulting curve may be markedly different from a static uniaxial stress-strain curve and can only be checked against a dynamic calculation. The air shock wave speeds are very high compared to the material wave velocity and the waves are relatively long compared to gage depths, so the initial compressive motion should be uniaxial, but after a time, effects from other parts of the test bed will be seen. Reflections from layers, waves from cratering regions and high shock pressure regions that develop through shock-shock interactions will all perturb the test bed in a three dimensional way. Therefore, only the compressive phase of the data is being considered.

Analysis of the dynamic stress-strain data shows different behavior in two different parts of the test bed, although large energy absorption in the soil is indicated. The air shock structure is not reproduced in the stress records from shallow gages and significant attenuation of the peak pressure is observed with depth.

1. "Misers Bluff Series; Phase II, Ground Shock and Airblast Measurements Data Report", Final Report, WES, M.P.N.-78-4, June 1978.
2. "Soil Strain Measurements on Misers Bluff - Phase II", DNA Topical Report, R. A. Shunk (unpublished).

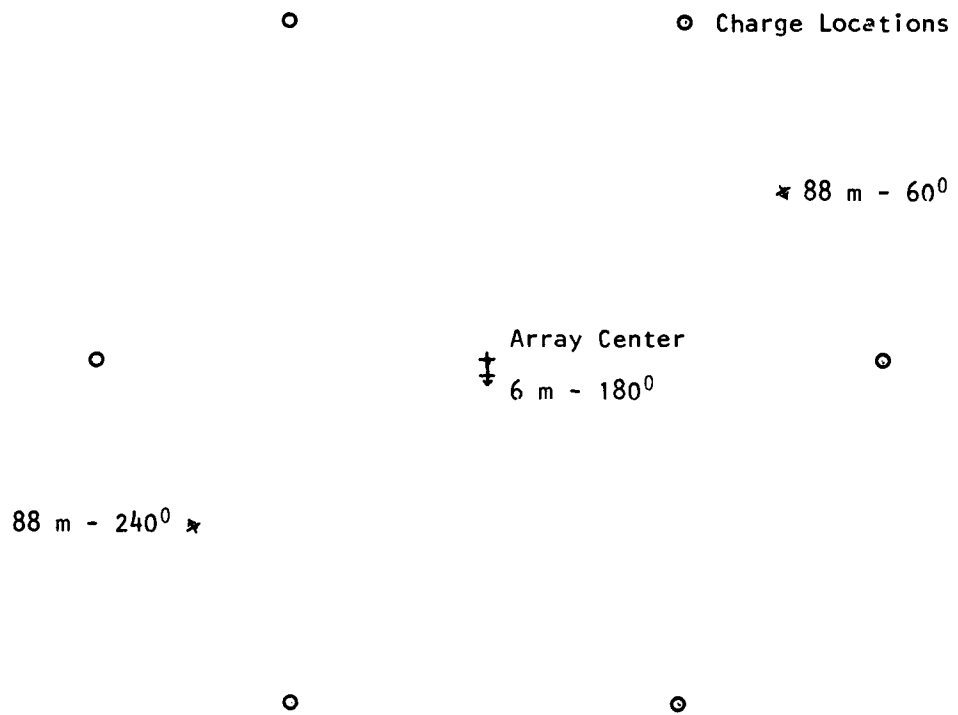


Figure 1. Measurement and charge locations for the stress-strain measurements on Misers Bluff-Phase II. Horizontal stresses are measured in the directions of the arrows at the measurement locations.

SECTION II

DYNAMIC STRESS-STRAIN MEASUREMENTS

The strain measurements were made with a telescoping spool gage (Reference 2) with a span of 2 cm. The output was derived from a linear variable differential transformer with a linear range of 5 cm. The stress measurements were made with the Waterways Experiment Station (WES) "SE" gage, a small diaphragm-type stress gage (Reference 3). The diaphragm deflection is detected by strain gages cemented to the diaphragm. All signals were recorded on magnetic tape as analogue voltages which were later digitized and plotted at WES.

The material in the upper meter of the test bed where these measurements were made was a weak aeolian soil with a void ratio of 40% (Reference 4).

Unfortunately, the return from the stress data was not as high as desired and some gages did not produce data for one reason or another. Thus, at several depths, only horizontal stress data are available. The data at 1.2 m depth and at 0.3 m depth at the 6 m - 180 station shows that the vertical stress is twice the horizontal stress. So to get the dynamic stress-strain curves in Figure 12, the horizontal stress was multiplied by two to get an estimate of the vertical stress. The supporting stress and strain records for 240 - 87.7 m are shown in Figures 7 through 11.

The curves in Figure 12 show the strain decreasing with depth. The peak strain is -17%, well within the gage range of -22% (negative strain

3. Ingram, T. D., "Development of a Free-Field Soil Stress Gage for Static and Dynamic Measurements," Technical Report No. 1-814, Feb. 1968, U.S. Army Engineer Waterways Experiment Station, CE, Vicksburg, Miss.
4. Jackson, Ed, "Geotechnical Investigation for Misers Bluff II" in the Misers Bluff Phase II Symposium Report, POR 7013, (unpublished), U.S. Army Engineer Waterways Experiment Station, Vicksburg, Miss.

is compressive). The peak stress is not falling off with depth. An increase in stress at 1.2 m over the stress at 0.6 m cannot be explained. The large open loop of the stress-strain curves indicates large energy absorption.

The data from the area at 6 m range, 180° from the array center will be examined next. The overpressure waveform is shown in Figure 13. The data from the two stress gages at 0.3 m are shown in Figures 14 and 15. A large attenuation in pressure is apparent. The strain record at 0.3 m is not credible because the form indicates gage failure and will not be discussed. The main point of showing these near surface gage records is to point out how the structure in the air pressure appears to be washed out by the soil or the combination of soil and stress gage interaction. A similar thing happened at 240° but one of the lower gages (Figure 7) seems to show the air pressure structure.

The response of the shallow stress gages to the multiple spikes in the air pressure waves is indicative of material response after the initial air shock loading that is not understood. For example, the air shock wave histories at both locations contain several spikes. At 87 m, 240° there are two very distinct spikes of about the same amplitude (Figure 2). The stress gage records at 0.3 m depth, Figure 4 and 5, show no indication of the second spike. There is a problem here in that the horizontal stress recorded is higher than the overpressure which is unlikely. The horizontal stress gages were oriented with the sensitive direction toward the nearest charge. A sharp third spike of about two thirds the amplitude of the first two appears in the pressure wave at about 23 msec. There is a rise in the vertical stress record at the correct time to represent this air pressure spike but it only goes to about 0.40 of the peak stress value. At 6 m - 180°, there is a somewhat similar effect where the first vertical stress rise in Figure 14 is about the same as the air pressure rise in Figure 13, about 2 Mpa. The air pressure wave decays slightly and two more distinct spikes follow in the air pressure record. These are reproduced in time in the stress record but very poorly in amplitude. The stress gage shows 3.1 Mpa compared to 9 Mpa for the third air shock. The horizontal stress gage in Figure 15 shows sharper rise times but lower amplitudes and in

both instances the second spike is lower than the first. Soil strain at 87 m, 240^0 is less than -10% when the second spike arrives. Soil strain at 6 m, 180^0 is probably on the order of -10% when the second spike arrives. Thus, some change occurs in the material and/or the stress gage which, after the material is compacted and partially unloaded in stress but not in strain, does not allow the stress gage to respond to the surface pressure less than 0.3 m away.

The initial soil stresses and accelerations are quite high near the surface and one can conjecture about differential motion between the outer protective steel ring of the stress gage and the less dense gage body. The ring is there to remove the cross axis sensitivity of the gage. (A soft rubbery material separates the two.) If this motion were significant, the stress gage body would be exposed to edge effects created by the ring that is supposed to protect it, causing a distorted waveform. Theoretically, this would only occur during the initial wavefront passage, but could have a lasting effect on gage response.

The dynamic stress-strain data for 180^0 - 6 m are shown in Figure 23 for three depths where stress measurements are available. They show an open loop response but have a stress cutoff unlike the data at 240^0 . There is a definite decrease in peak compressive strain with depth. The supporting data are shown in Figures 16 through 22.

SECTION III

CONCLUSIONS AND RECOMMENDATIONS

How much the different material reactions in the two measurement locations depend on the peak overpressure, overpressure waveforms and the interactive material properties cannot be sorted out by inspecting these data. However, it is clear that a large amount of energy is dissipated in this material during shock loading. The stress gage and material response to multiple shock loadings needs to be explained if the stress data are to have much value.

Modeling of the material and some high pressure, one dimensional shock loading tests of similar materials in a realistically scaled facility could be used to get some additional information on dynamic stress-strain behavior. A one dimensional experiment would be valuable where stress, strain and acceleration-velocity can be measured with multiple step surface loads of on the order of 2 to 10 Mpa. A one dimensional calculational effort using a material model structured around the MISERS BLUFF soil might give the clues necessary to explain the stress data obtained on MISERS BLUFF, Phase II, Test 2.

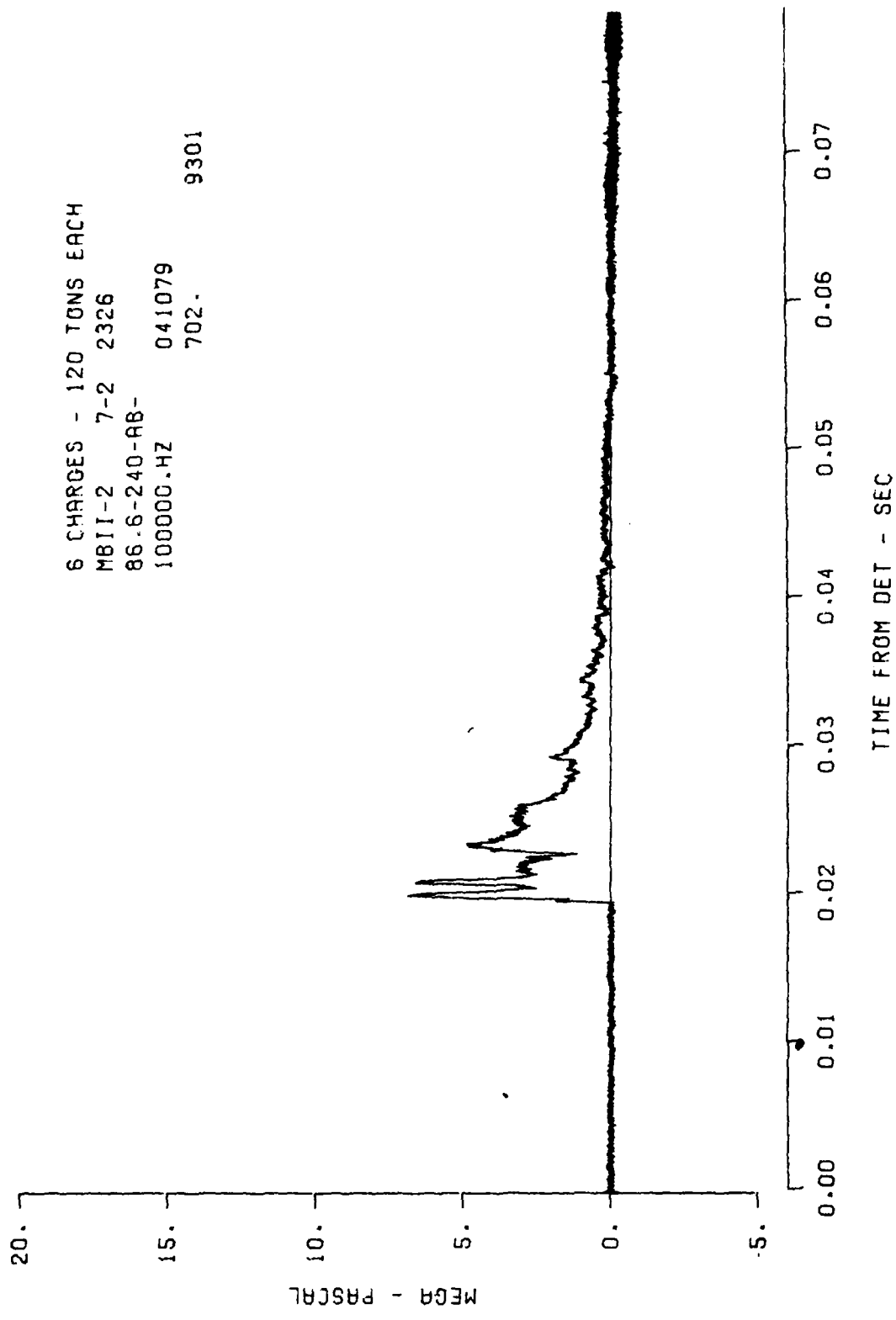


Figure 2. Surface overpressure near the stress-strain measurement locations at 87 m, 240° azimuth.



Figure 3. Diaphragm stress gages partially uncovered for measuring vertical and horizontal stress.

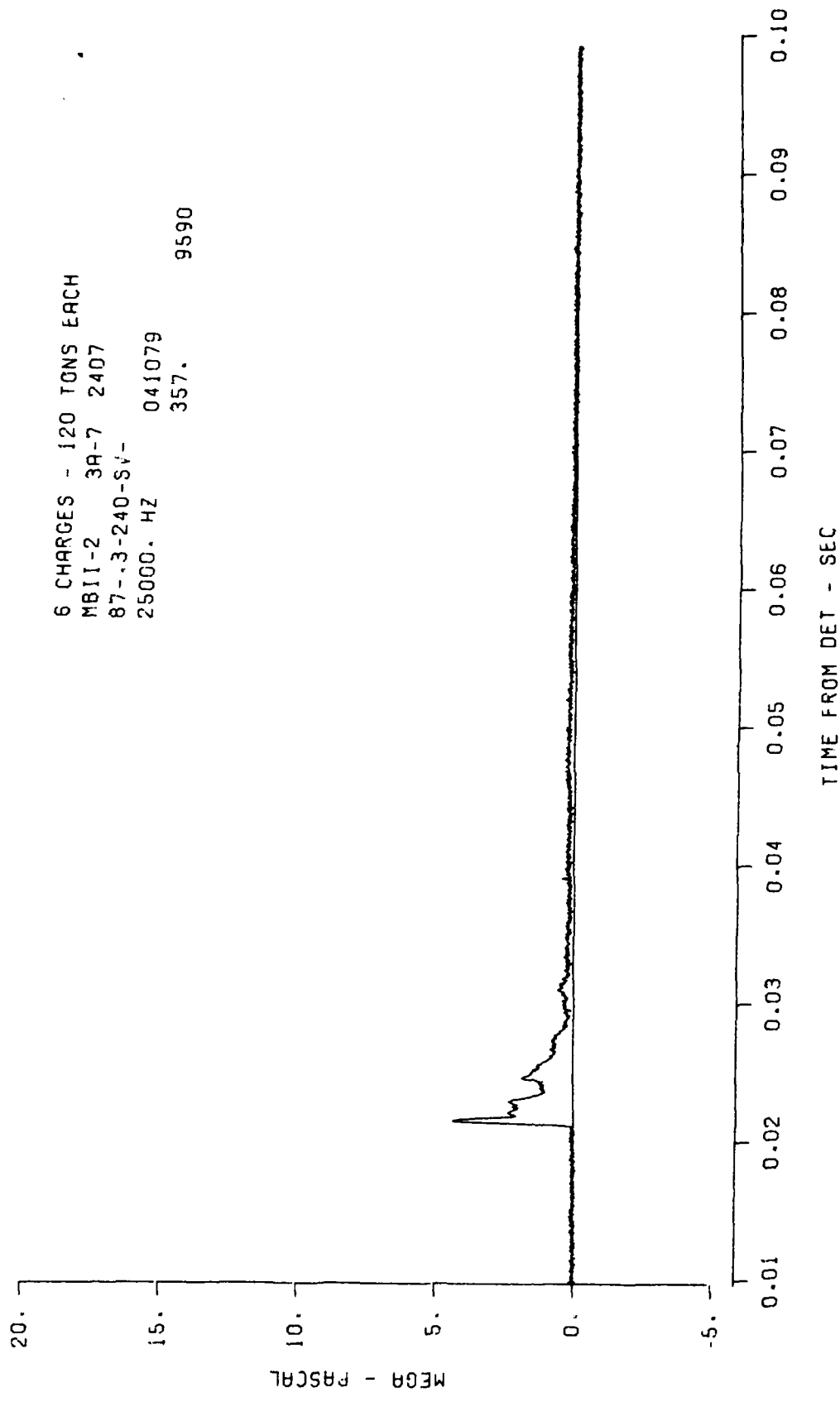


Figure 4. Vertical stress at 87 m, 0.3 m depth and 240° azimuth.

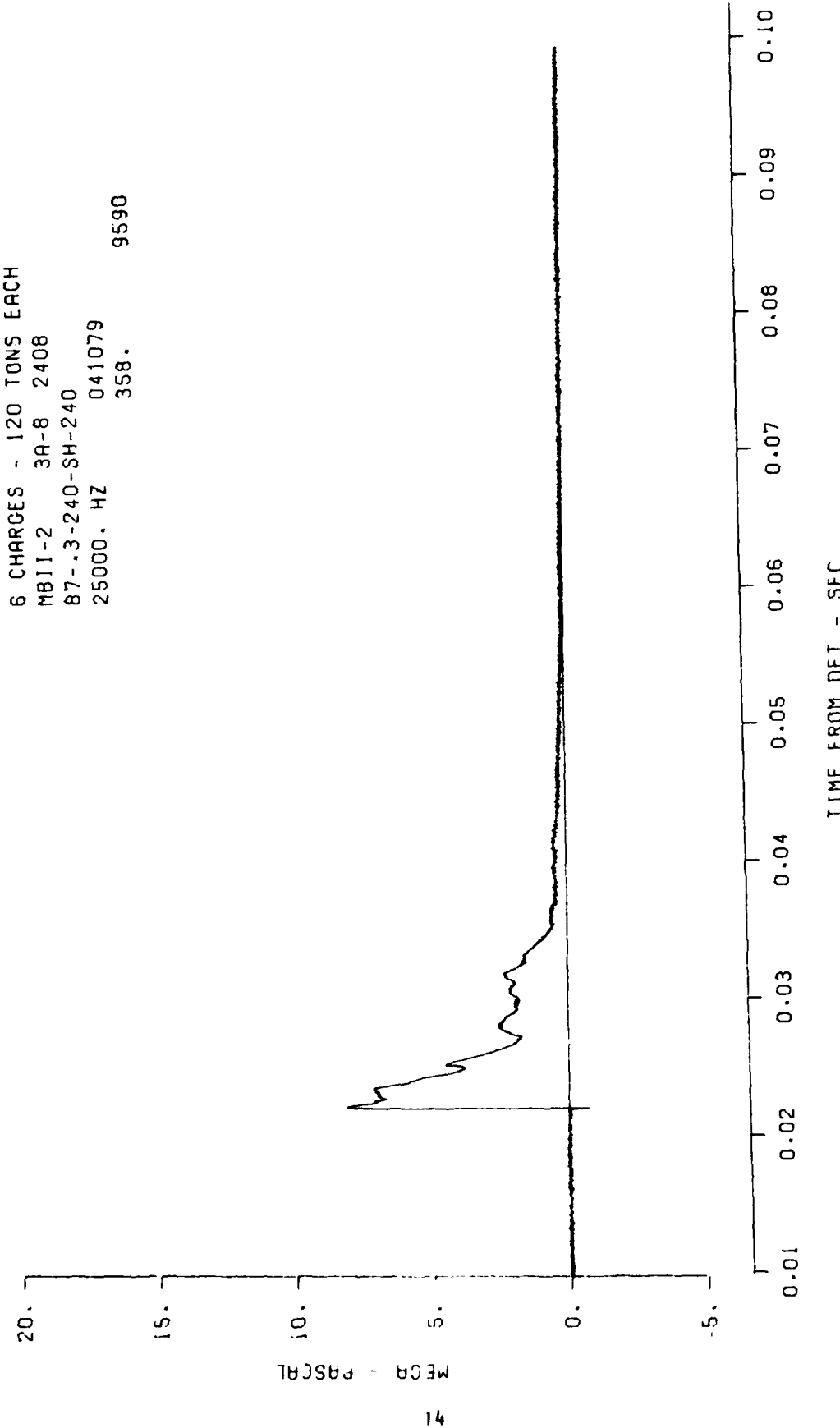


Figure 5. Horizontal stress at 87 m, 0.3 m depth and 240° azimuth.

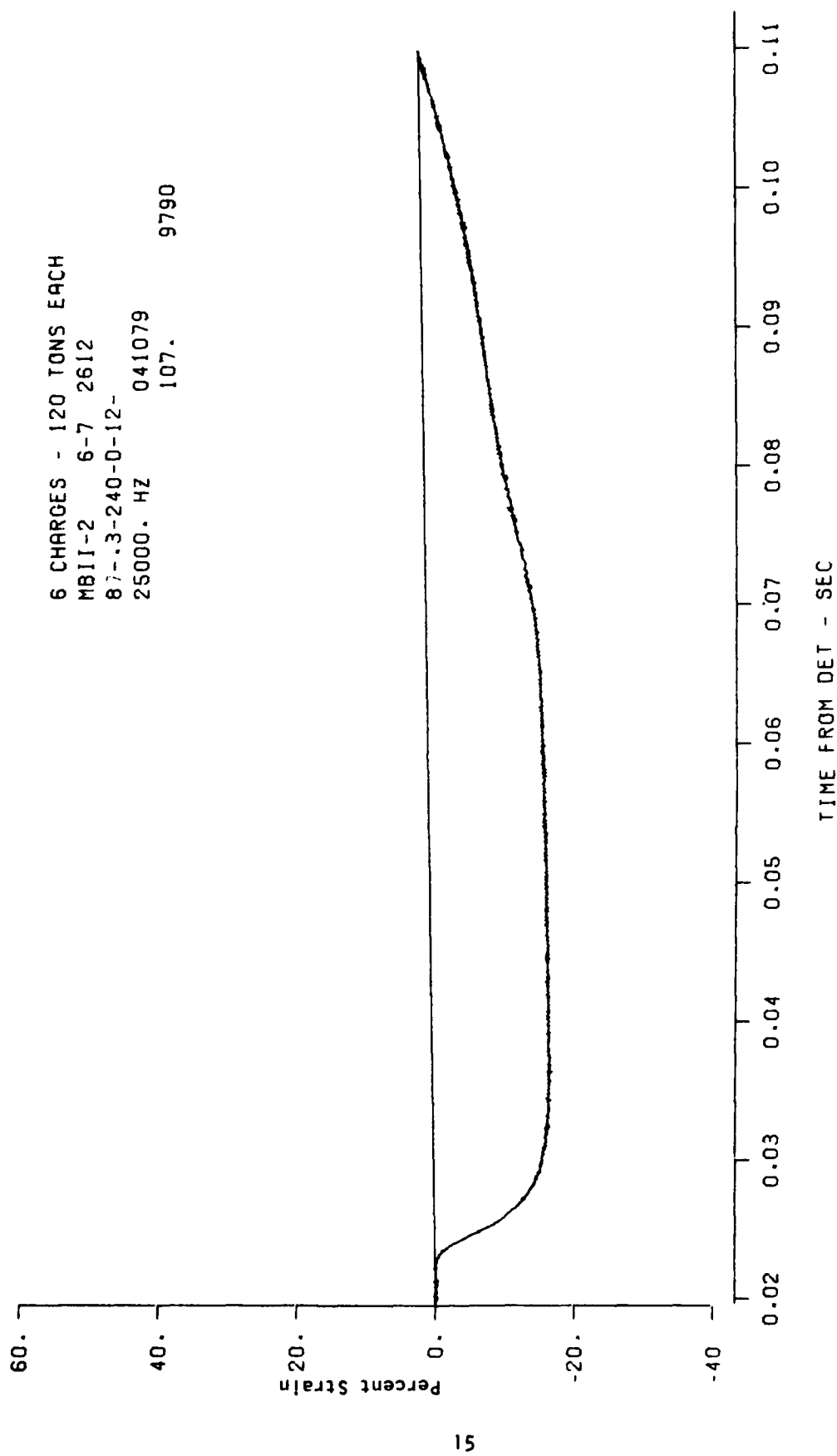


Figure 6. Vertical strain at 87 m, 0.3 m depth and 240° azimuth.

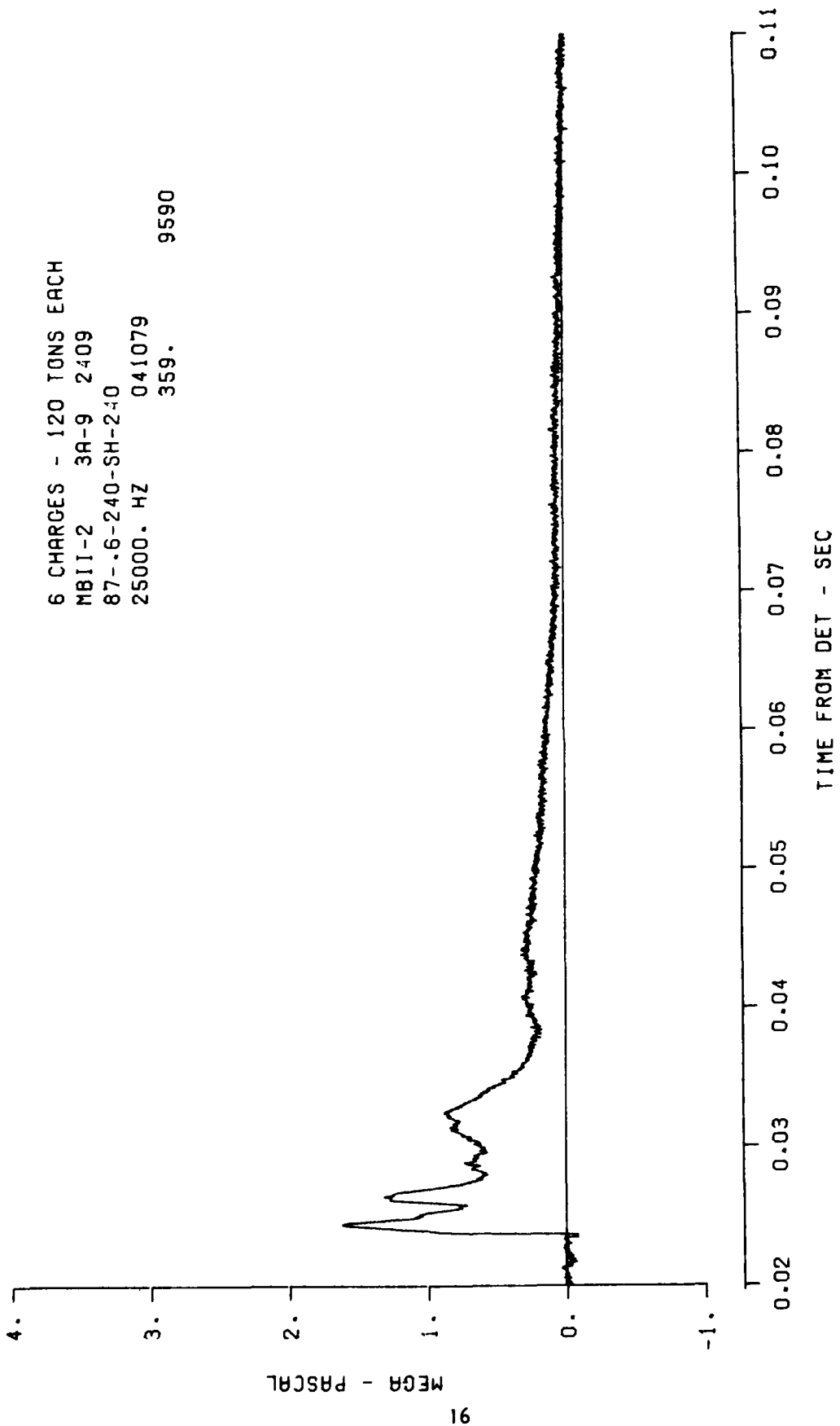


Figure 7. Horizontal stress at 87 m, 0.6 m depth and 240° azimuth.

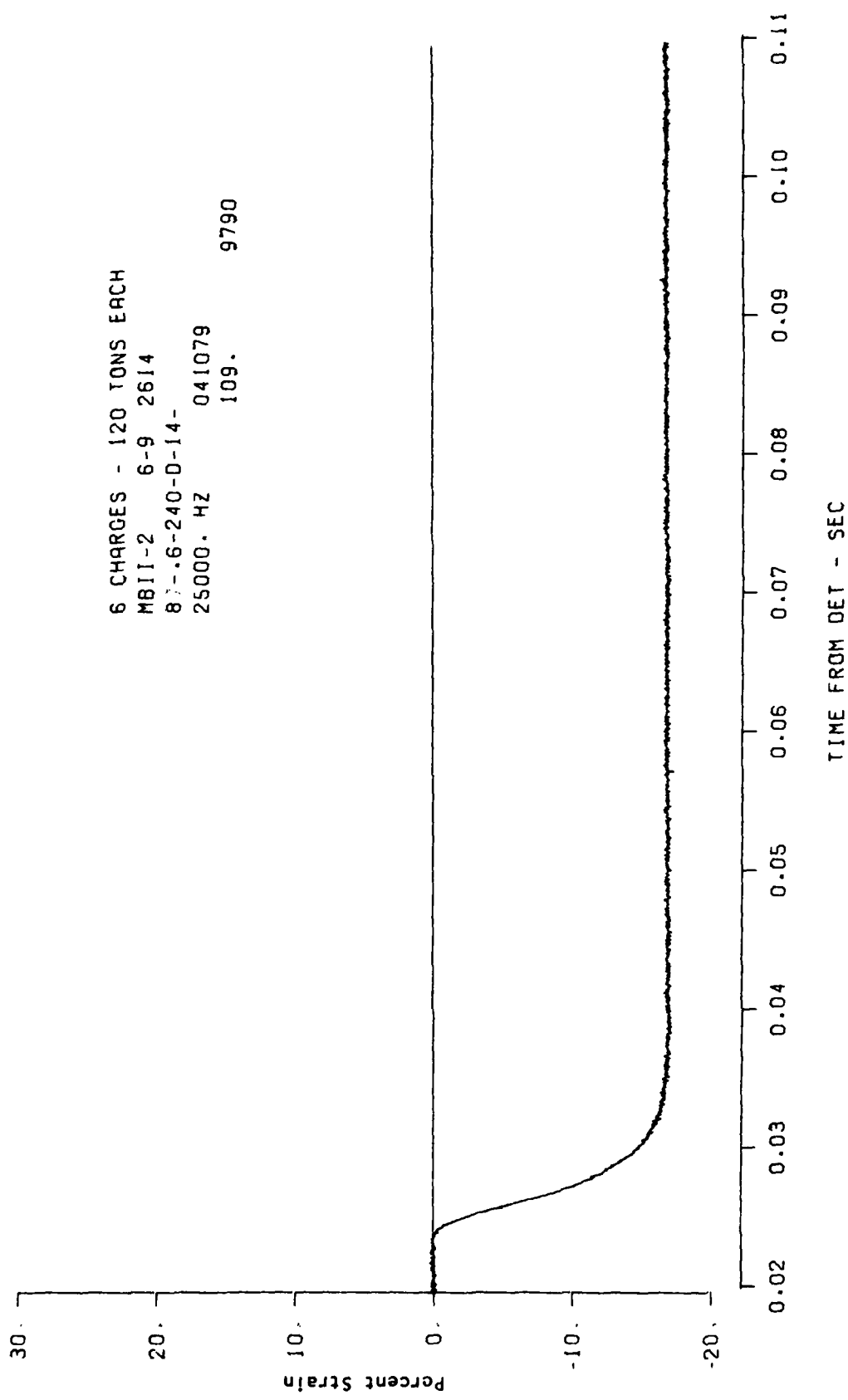


Figure 8. Vertical strain at 87 m, 0.6 m depth and 240° azimuth.

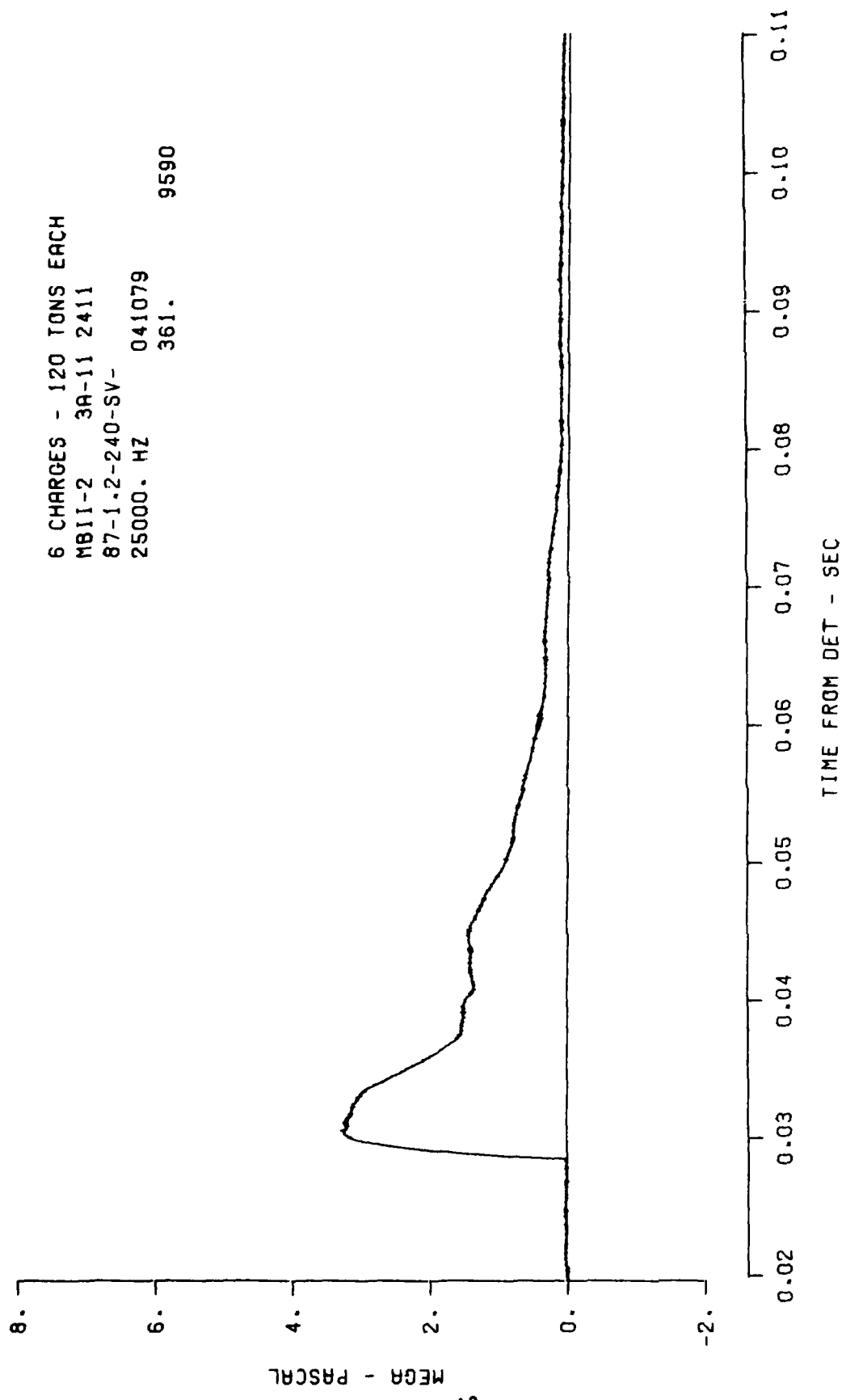


Figure 9. Vertical stress at 87 m, 1.2 m depth and 240° azimuth.

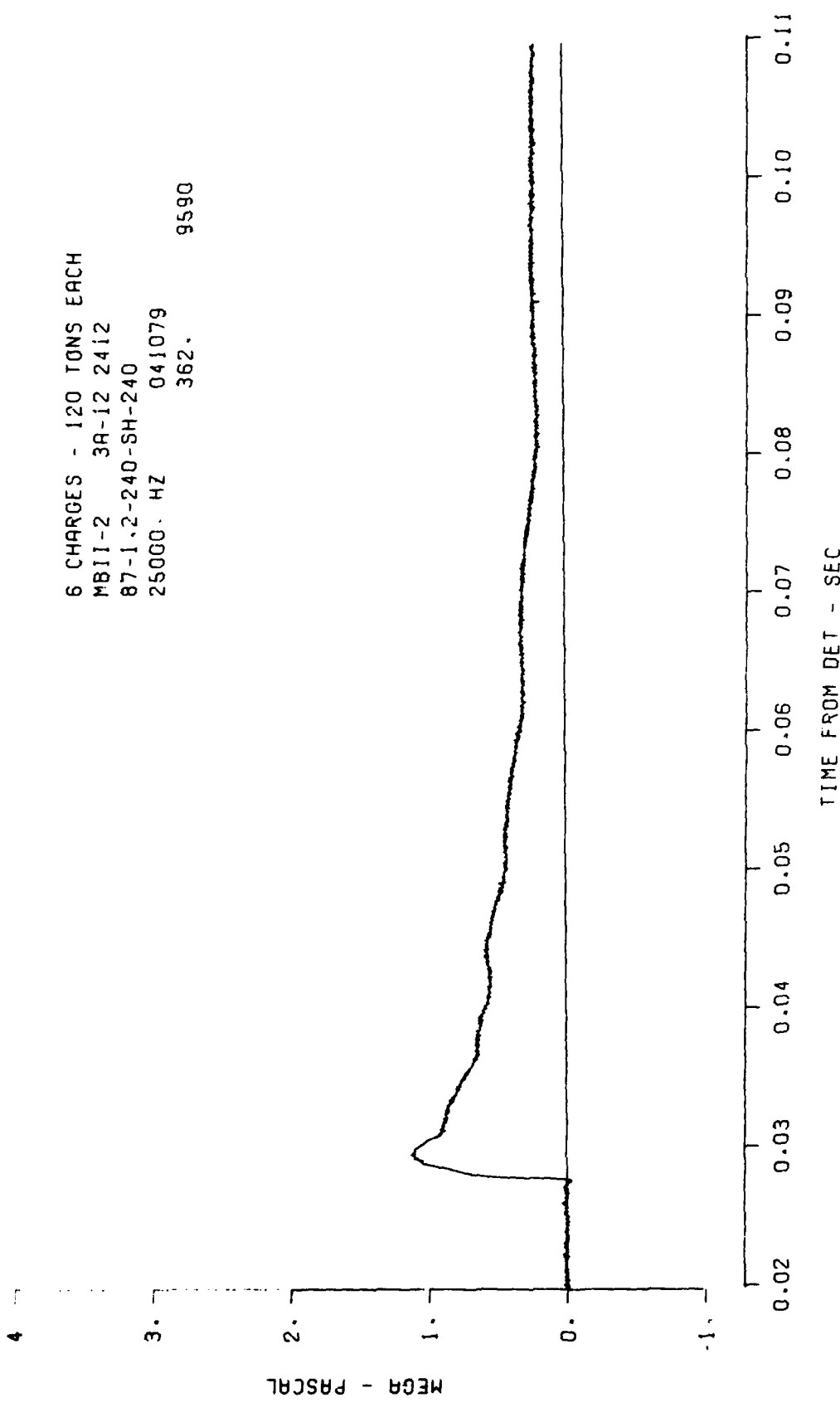


Figure 10. Horizontal stress at 87 m, 1.2 m depth and 240° azimuth.

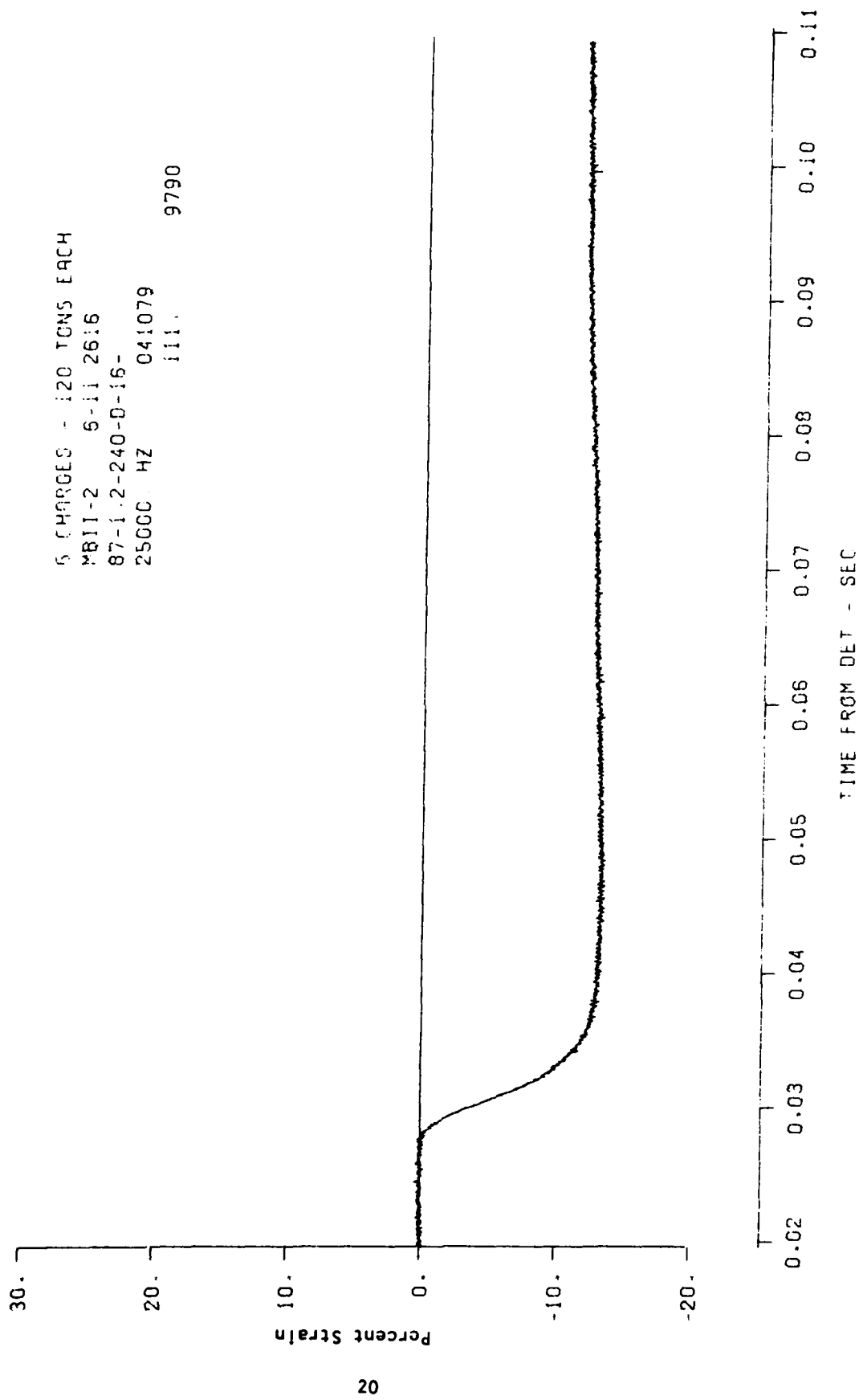


Figure 11. Vertical strain at 87 m, 1.2 m depth and 240° azimuth.

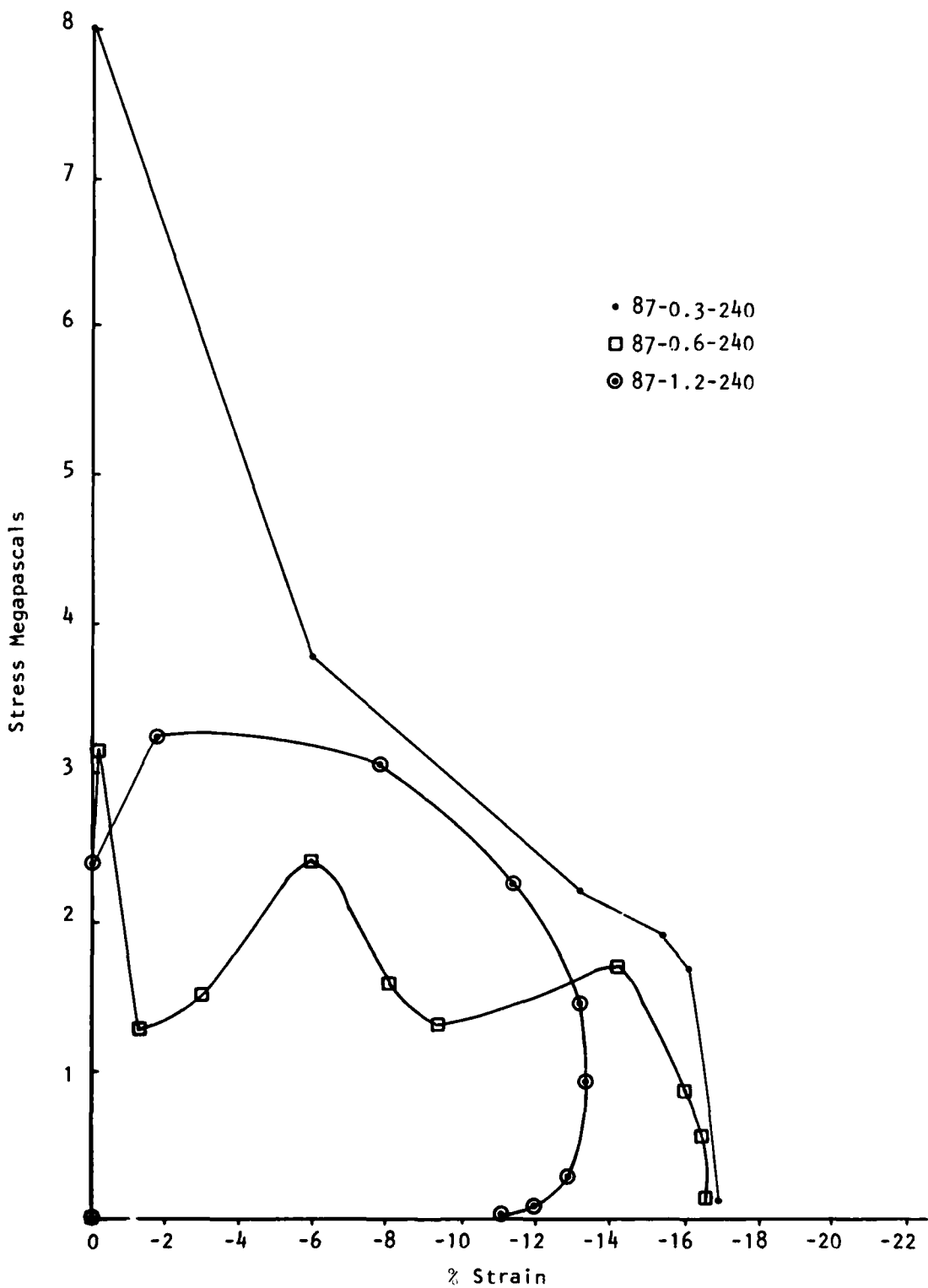


Figure 12. Dynamic stress-strain curves for three depths at 87 m, 240° azimuth.

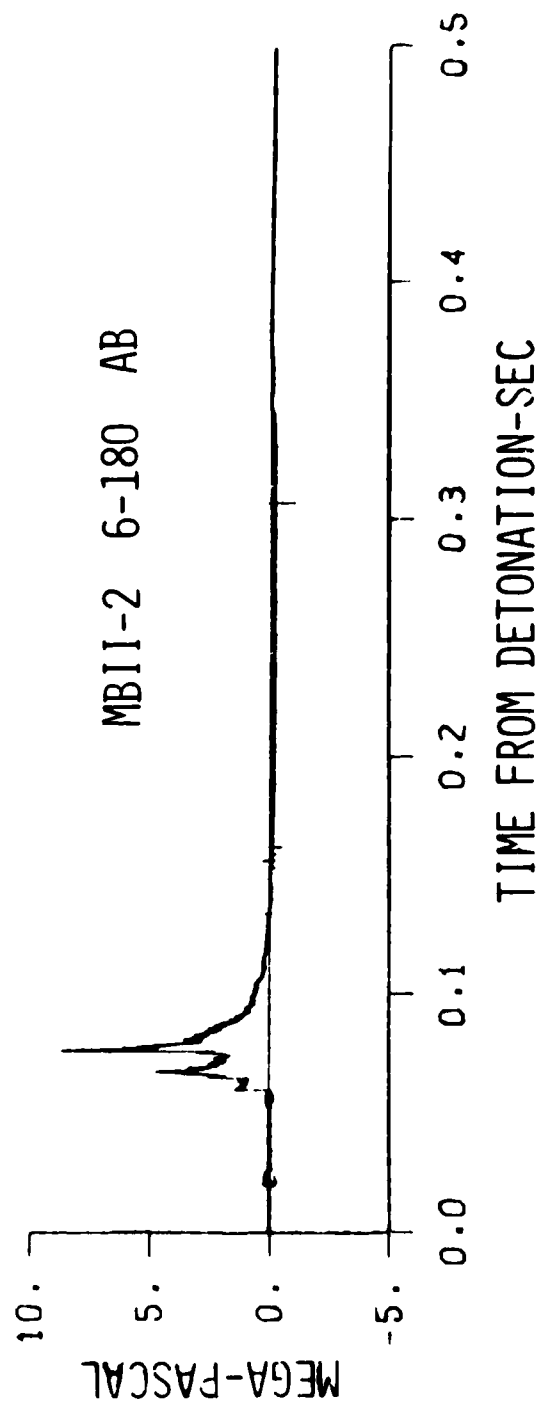


Figure 13. Air blast wave form at 180^0 and 6 m from center of the array over strain gage emplacement.

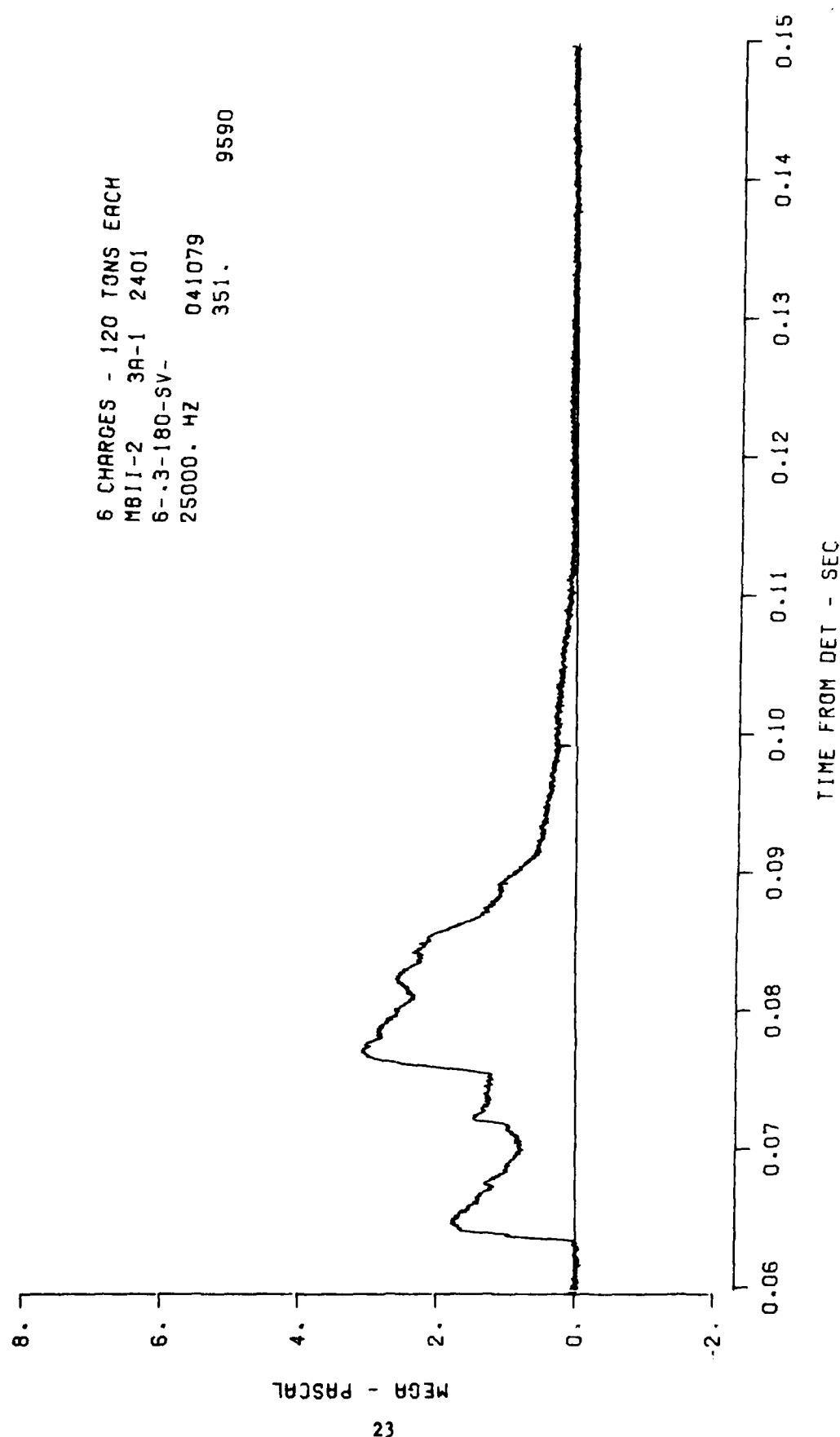


Figure 14. Vertical stress at 6 m, 0.3 m depth and 180° azimuth.

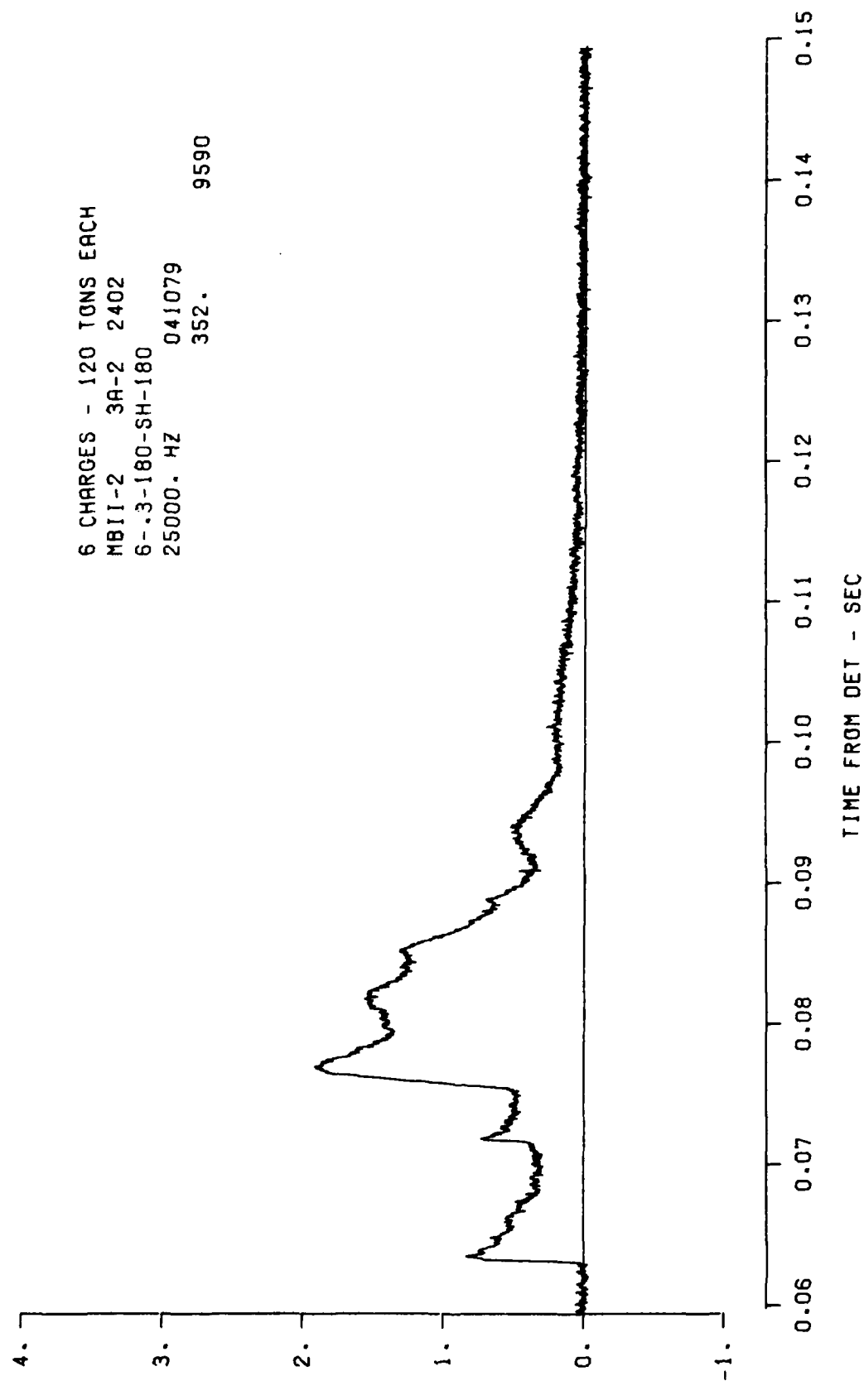


Figure 15. Horizontal stress at 6 m, 0.3 m depth and 180° azimuth.

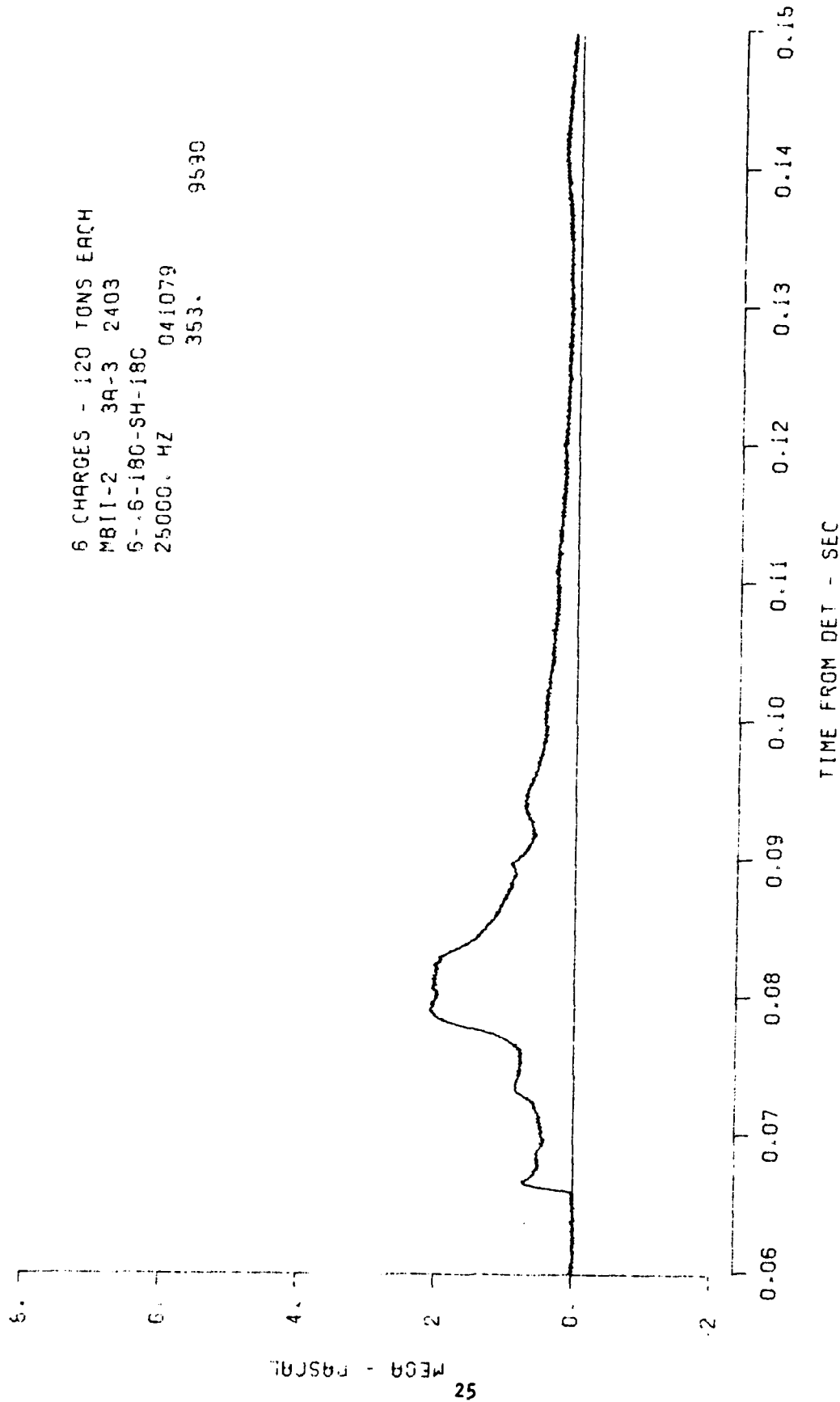


Figure 16. Horizontal stress at 6 m, 0.6 m depth and 180^0 azimuth.

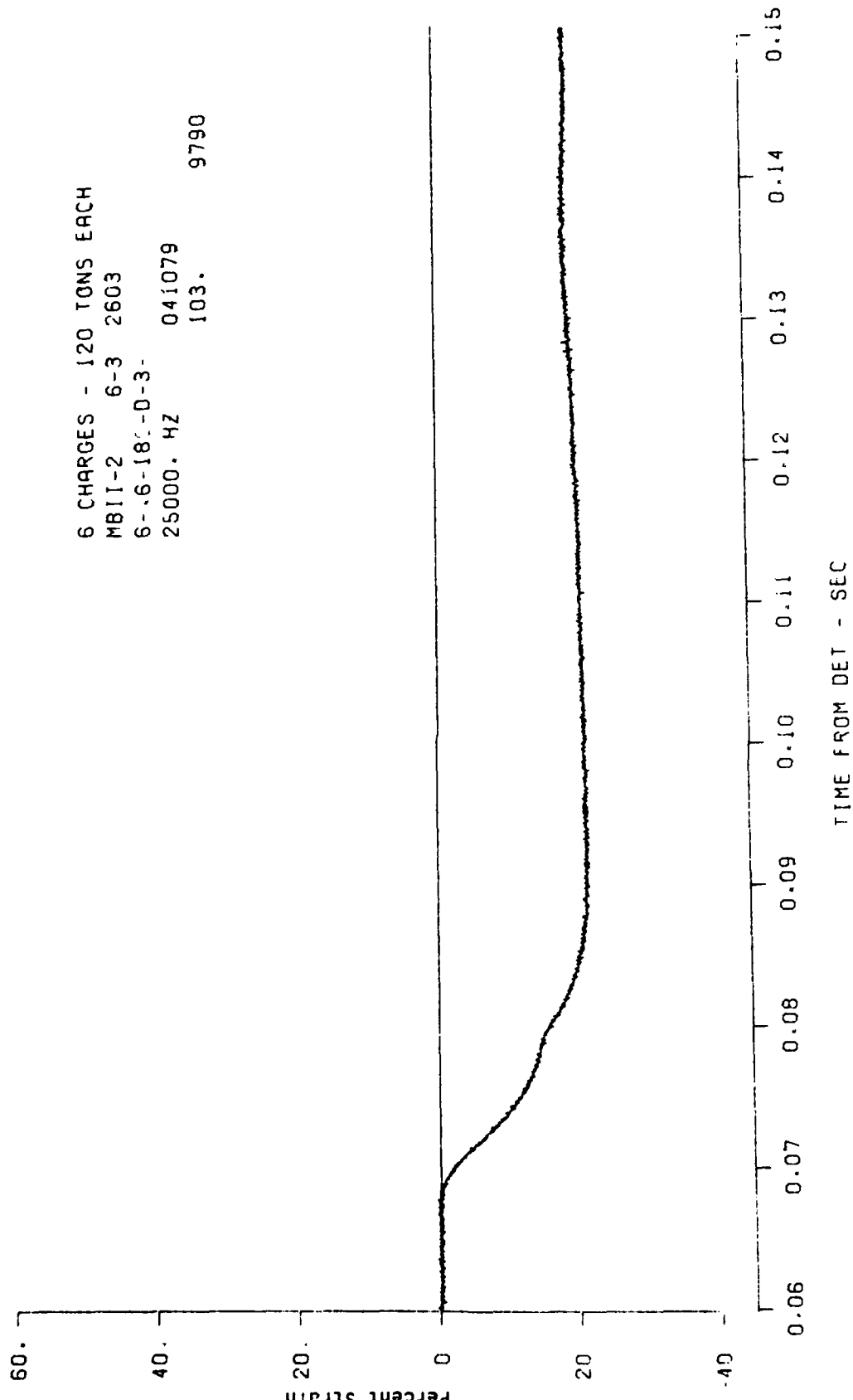


Figure 17. Vertical strain from 6 m, 0.6 m depth and 180° azimuth.

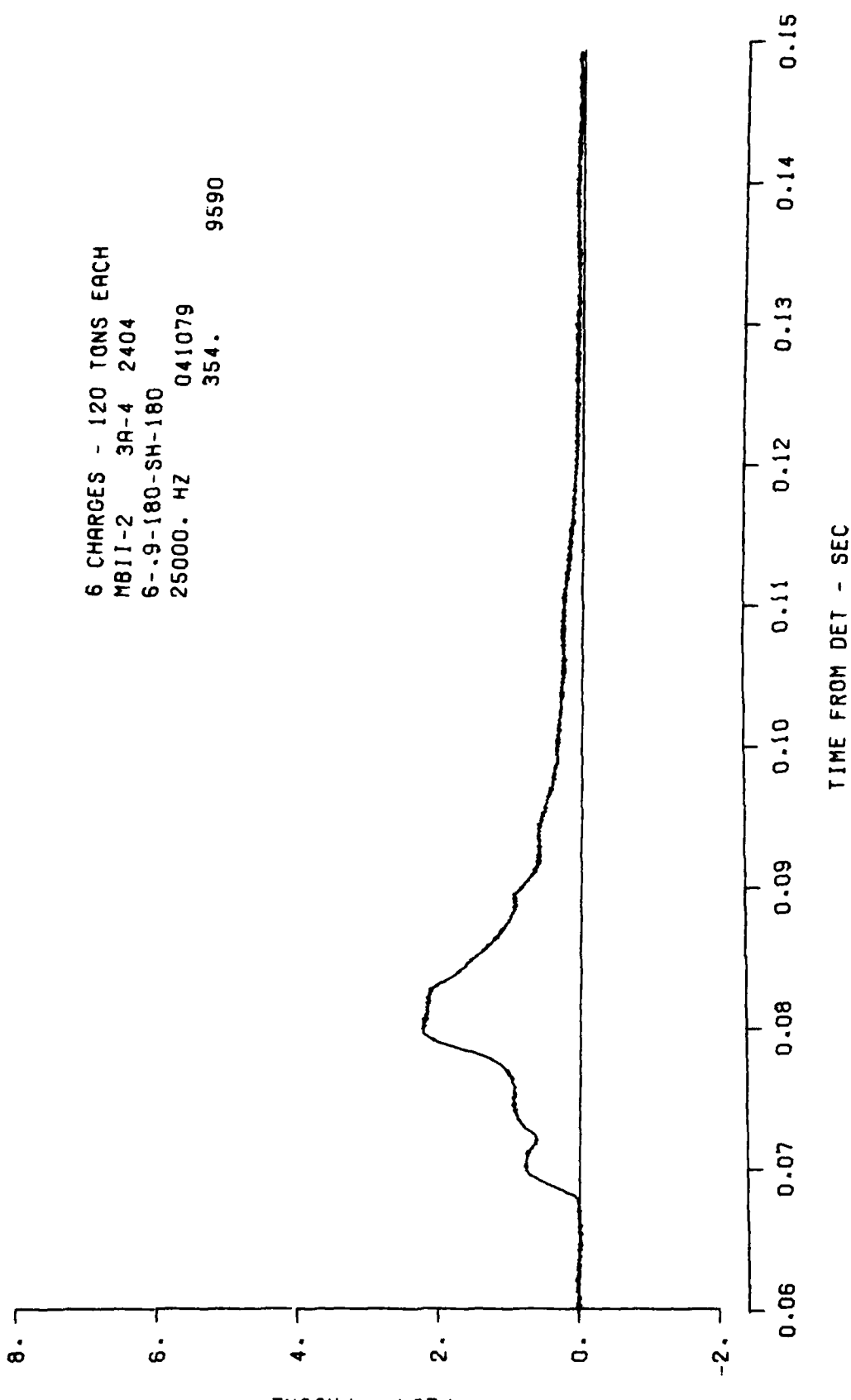


Figure 18. Horizontal stress from 6 m, 0.9 m depth and 180^0 azimuth.

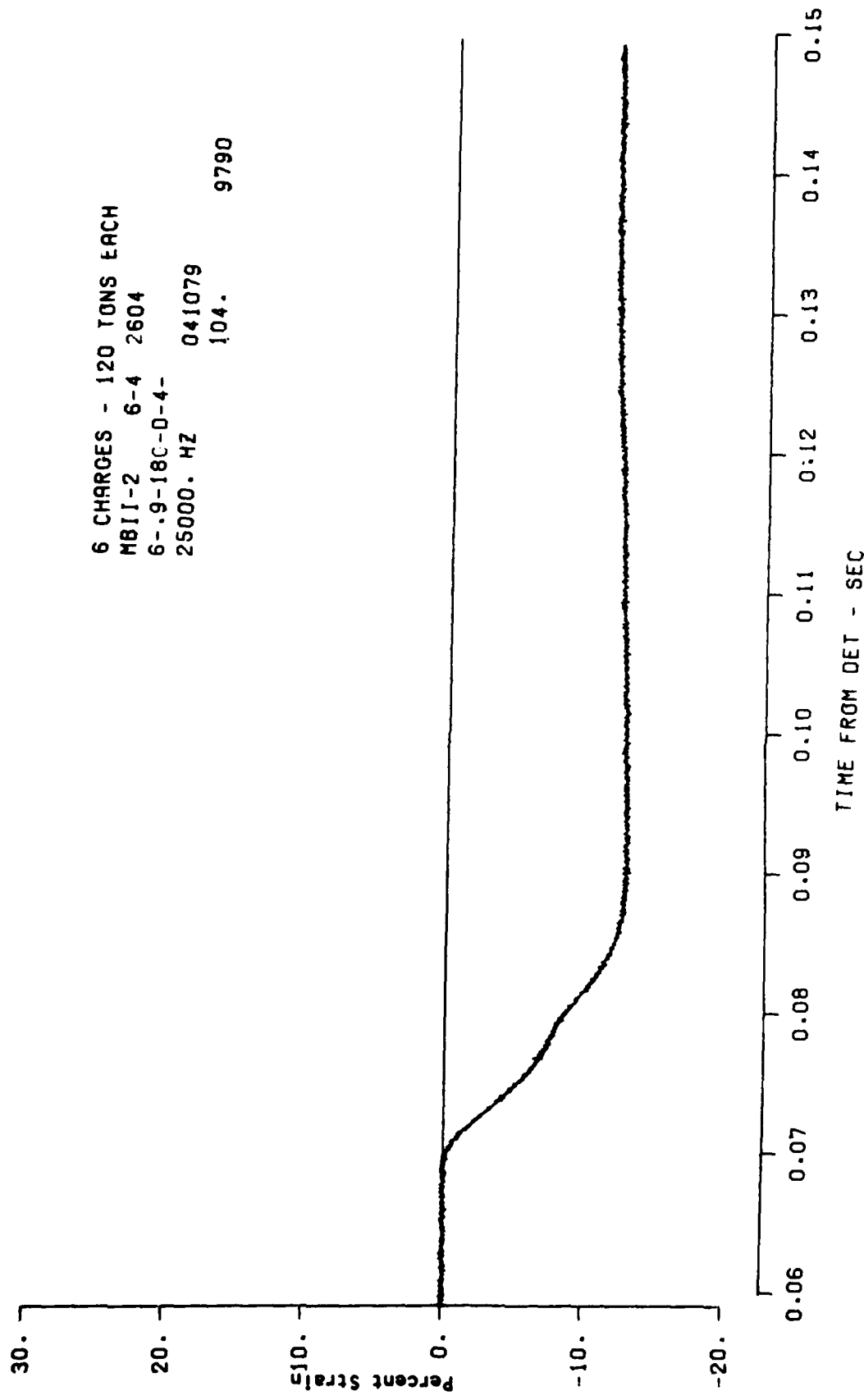


Figure 19. Vertical strain from 6 m, 0.9 m depth and 180° azimuth.

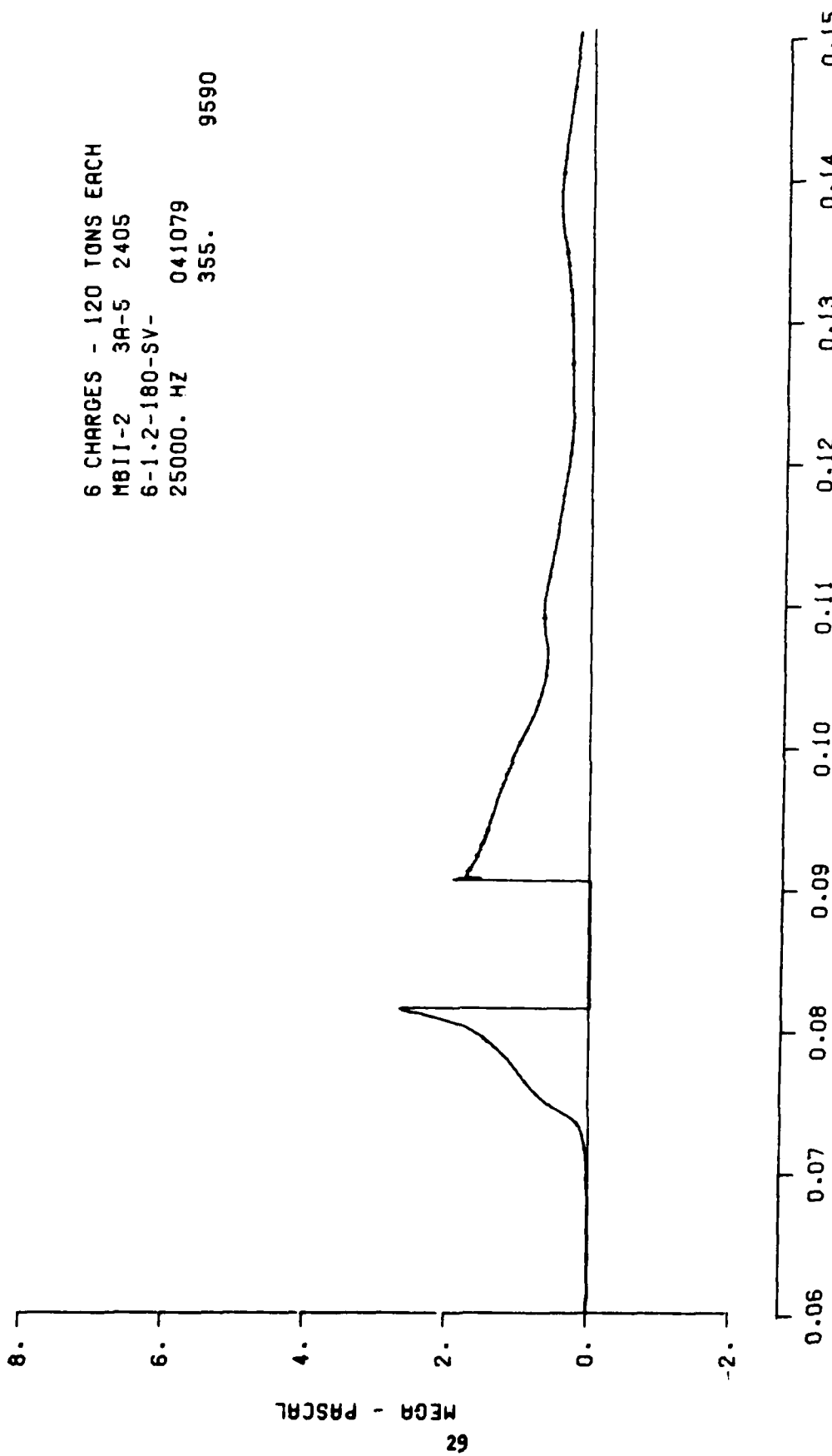


Figure 20. Vertical stress from 6 m, 1.2 m depth and 180° azimuth.

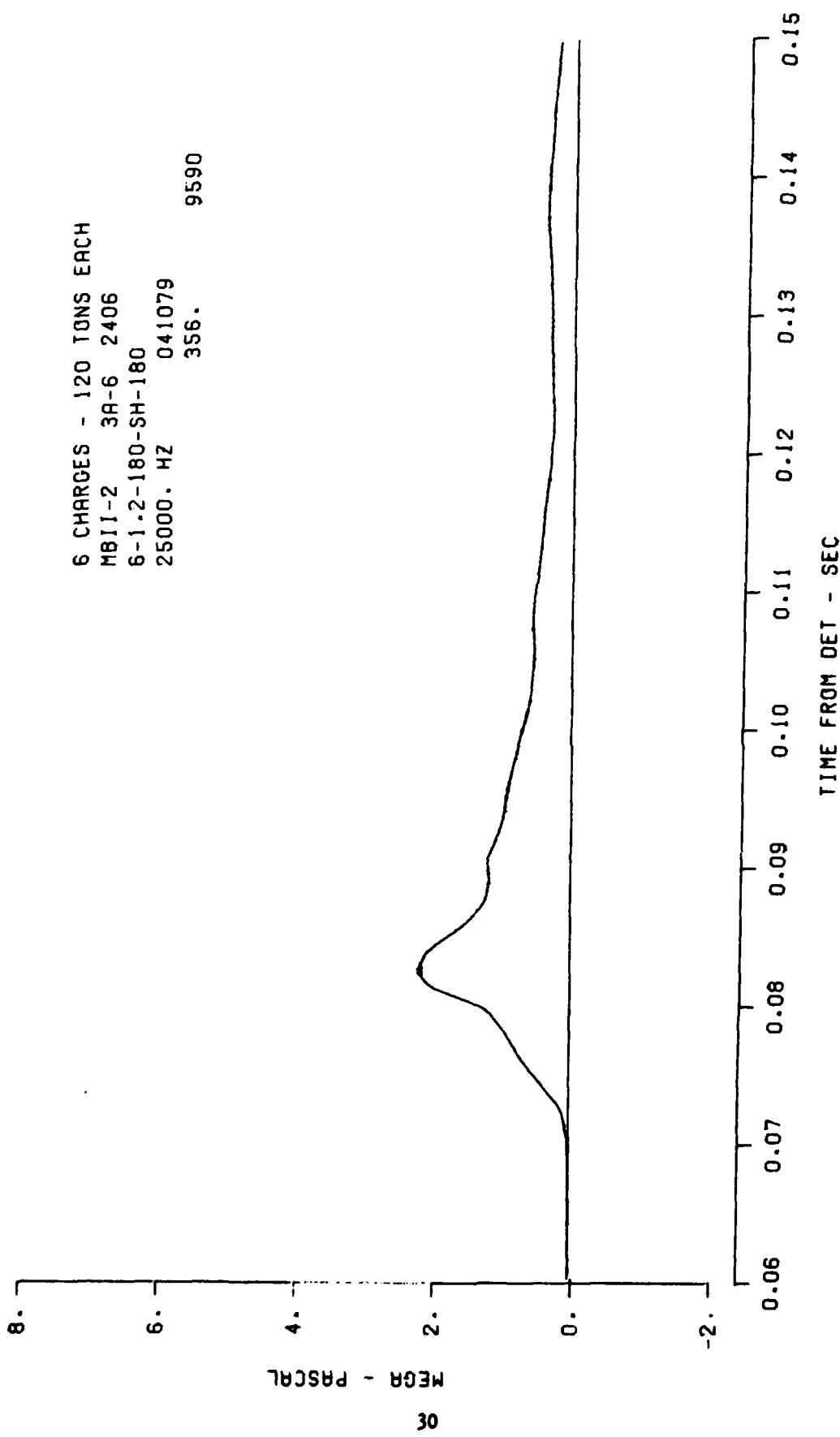


Figure 21. Horizontal stress at 6 m, 1.2 m depth and 180° azimuth.

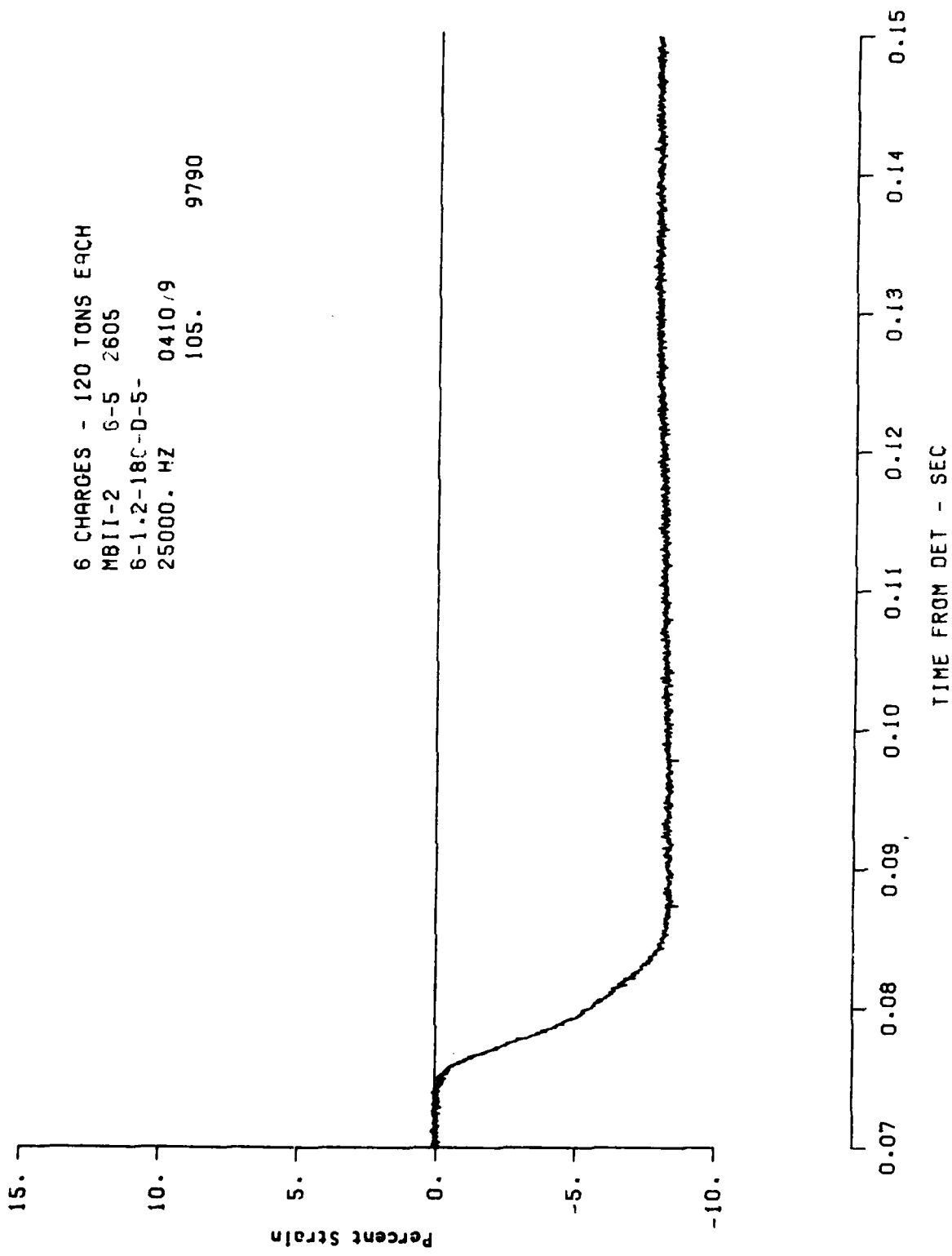


Figure 22. Vertical strain at 6 m, 1.2 m depth and 180° azimuth.

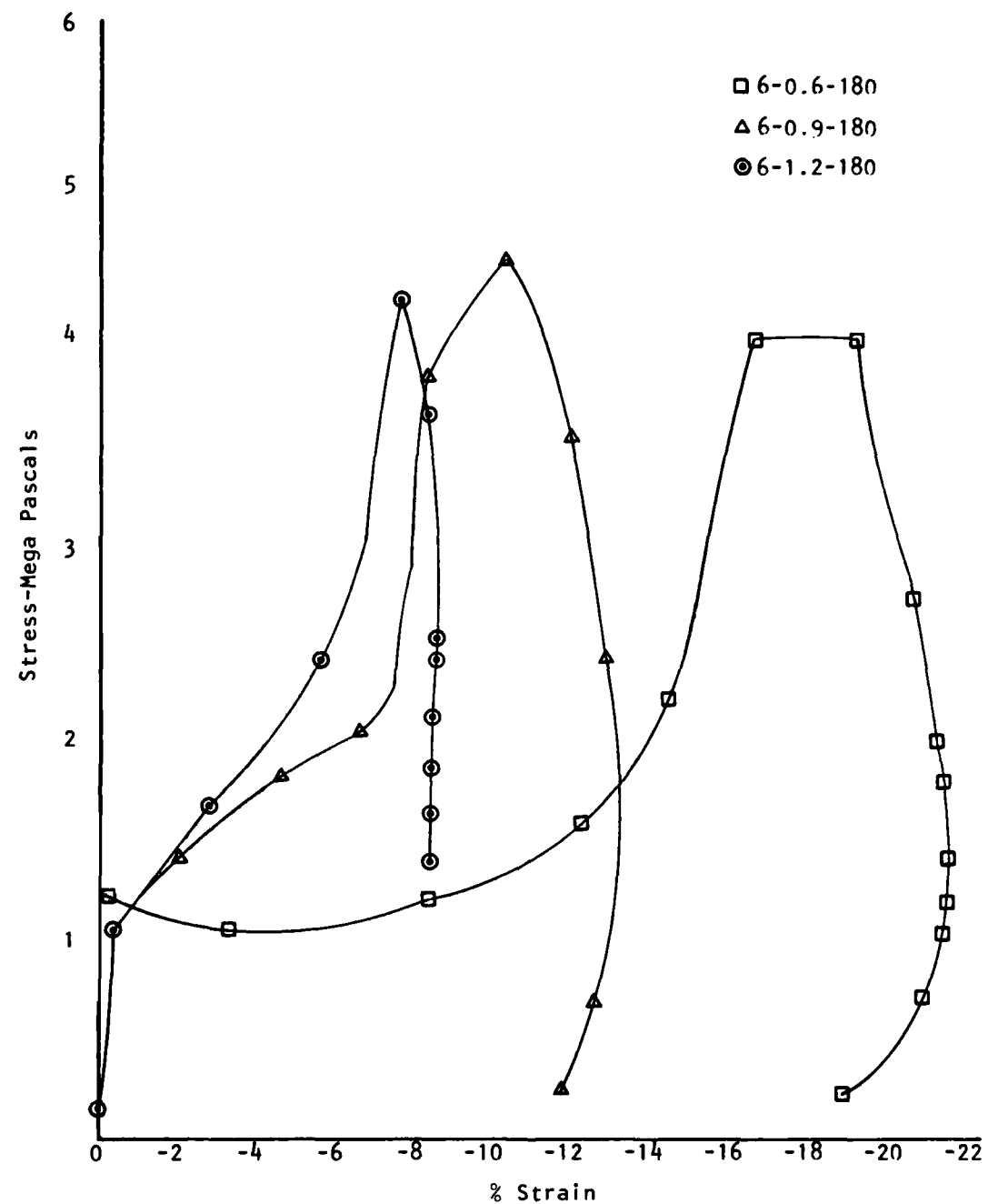


Figure 23. Dynamic stress-strain curves for three depths at 6 m, 180° azimuth.

DISTRIBUTION LIST

DEPARTMENT OF DEFENSE

Assistant to the Secretary of Defense
Atomic Energy
ATTN: Executive Assistant

Defense Technical Information Center
12 cy ATTN: DD

Defense Nuclear Agency
ATTN: DDST
ATTN: SPTD
4 cy ATTN: TITL
2 cy ATTN: SPSS

Field Command
Defense Nuclear Agency
ATTN: FCT
ATTN: FCTMOF
ATTN: FCPR

Field Command
Defense Nuclear Agency
ATTN: FCPRL

Undersecretary of Def. for Rsch. & Engrg.
ATTN: Strategic & Space Systems (OS)

DEPARTMENT OF THE ARMY

Harry Diamond Laboratories
Department of the Army
ATTN: DELHD-N-P
ATTN: DELHD-I-TL

U.S. Army Ballistic Research Labs.
ATTN: DRDAR-BLT, W. Taylor
ATTN: DRDAR-TSB-S
ATTN: DRDAR-BLE, J. Keefer
ATTN: DRDAR-BLV

U.S. Army Cold Region Res. Engr. Lab.
ATTN: CRREL-EM

U.S. Army Engr. Waterways Exper. Station
ATTN: L. Ingram
ATTN: G. Jackson
ATTN: J. Strange
ATTN: J. Ingram
ATTN: W. Flathau
ATTN: F. Hanes
ATTN: Library

U.S. Army Nuclear & Chemical Agency
ATTN: Library

DEPARTMENT OF THE NAVY

Naval Surface Weapons Center
ATTN: Code F31

DEPARTMENT OF THE AIR FORCE

Space & Missile Systems Organization
Air Force Systems Command
ATTN: DEB

DEPARTMENT OF THE AIR FORCE (Continued)

Air Force Weapons Laboratory
Air Force Systems Command
ATTN: DED, R. Matalucci
ATTN: DE, M. Plamondon
ATTN: DEX, J. Renick
ATTN: DES-C, R. Henny
ATTN: SUL
ATTN: DEX

Space & Missile Systems Organization
Air Force Systems Command
ATTN: MMH
ATTN: MNNH

DEPARTMENT OF DEFENSE CONTRACTORS

Acurex Corp.
ATTN: K. Triebes

Aerospace Corp.
ATTN: P. Mathur
ATTN: Technical Information Services

Agbabian Associates
ATTN: M. Agbabian

Analytic Services, Inc.
ATTN: G. Hesselbacher

Applied Theory, Inc.
2 cy ATTN: J. Trulio

Artec Associates, Inc.
ATTN: D. Baum
ATTN: S. Gill

AVCO Research & Systems Group
ATTN: Library A830

BDM Corp.
ATTN: T. Neighbors
ATTN: A. Lavagnino
ATTN: Corporate Library

BDM Corp.
ATTN: R. Hensley

Boeing Co.
ATTN: B. Lempriere
ATTN: Aerospace Library
ATTN: R. Carlson

California Research & Technology, Inc.
ATTN: K. Kreyenhagen
ATTN: Library

Civil Systems, Inc.
ATTN: J. Bratton

DEVELCO, Inc.
ATTN: L. Rorden

EG&G Washington Analytical Services Center, Inc.
ATTN: Library

DEPARTMENT OF DEFENSE CONTRACTORS (Continued)

Electromechanical Sys. of New Mexico, Inc.
ATTN: R. Shunk

Eric H. Wang
Civil Engineering Rsch. Fac.
ATTN: N. Baum

General Electric Company-TEMPO
ATTN: DASIAC
ATTN: J. Shoutens

H-Tech Labs, Inc.
ATTN: B. Hartenbaum

Merritt CASES, Inc.
ATTN: J. Merritt
ATTN: Library

Physics International Co.
ATTN: Technical Library
ATTN: L. Behrmann
ATTN: E. Moore
ATTN: F. Sauer

R & D Associates
ATTN: R. Port
ATTN: Technical Information Center
ATTN: J. Carpenter
ATTN: W. Wright, Jr.
ATTN: J. Lewis
ATTN: A. Kuhl
10 cy ATTN: A. Latter
ATTN: C. MacDonald

R & D Associates
ATTN: H. Cooper

DEPARTMENT OF DEFENSE CONTRACTORS (Continued)

Science Applications, Inc.
ATTN: Technical Library

Science Applications, Inc.
ATTN: K. Sites

SRI International
ATTN: B. Gasten/P. De Carli
ATTN: G. Abrahamson

Systems, Science & Software, Inc.
ATTN: T. Cherry
ATTN: Library
ATTN: D. Grine
ATTN: T. Riney

Tetra Tech, Inc.
ATTN: L. Hwang
ATTN: Library

TRW Defense & Space Sys. Group
ATTN: P. Bhutta
ATTN: Technical Information Center
ATTN: D. Baer
ATTN: R. Plebush
2 cy ATTN: P. Dai
ATTN: I. Alber

TRW Defense & Space Sys. Group
ATTN: E. Wong

Weidlinger Assoc., Consulting Engineers
ATTN: M. Baron